# Development of an empirical chart datum model for a region of the Southwest Atlantic Ocean

María Florencia de Azkue[1,2]*, Enrique Eduardo D'Onofrio[3], Luciano Banegas[1]

[1] Departamento Oceanografía, Servicio de Hidrografía Naval (SHN) (Av. Montes de Oca 2124 - Ciudad Autónoma de Buenos Aires - Código Postal C1270ABV - Argentina)

[2] Escuela de Ciencias del Mar, Facultad de la Armada, Universidad de La Defensa Nacional (Av. Antártida Argentina 425, Ciudad Autónoma de Buenos Aires; Código Postal: C1104AAD - Argentina)

[3] Facultad de Ingeniería, Universidad de Buenos Aires (Av. Paseo Colón 850 - Ciudad Autónoma de Buenos Aires - Código Postal: C1063ACV - Argentina)

* Corresponding author: maria.azkue@mindef.gov.ar

## ABSTRACT

The datum for sounding reduction is a permanently fixed surface, to which the depths displayed on the nautical charts and the tide tables heights refer. The International Hydrographic Organization recommends adopting the lowest astronomical tide as a chart datum, although its calculation can be complex because it varies both spatially and temporally. The ever increasing accuracy of 3D positioning with Global Navigation Satellite Systems requires that the chart datum is referenced to the ellipsoid WGS84. The aims of this paper are to calculate the lowest astronomical tide and to develop an empirical model to determine the distance between the lowest astronomical tide and the WGS84 ellipsoid, for a region of the Southwest Atlantic Ocean between latitudes 36°S and 54°S and longitude 54°W, on a 5km x 5km grid. Harmonic constants from the Centre for Topographic studies of the Oceans and Hydrosphere are used to calculate the lowest astronomical tide. To refer it to the WGS84 ellipsoid, results from mean sea level models and along-track sea level heights provided by Archiving, Validation and Interpretation of Satellite Oceanographic data are utilized. The final product has been designed for open waters and will be useful both for the development of relevant marine activities in the area, as well as to increase the efficiency of hydrographic surveys while contributing to more precise navigation in critical areas.

**Descriptors:** Lowest astronomical tide, WGS84 ellipsoid, Sounding measure.

## INTRODUCTION

The chart datum (CD) is a permanently fixed surface, to which the depths displayed on the nautical charts and the tide tables heights refer. The 3/1919 resolution of the International Hydrographic Organization (IHO) suggests that the lowest astronomical tides height (LAT) must be used as CD in areas with tidal ranges greater than 0.30m (IHO, 2010). The LAT is defined as the lowest astronomical tide

level which can be predicted to occur under average meteorological conditions and under any combination of astronomical conditions. Thereby a water level below LAT can only occur due to meteorological effects. IHO (2010) recommended that LAT must be calculated either over a minimum period of 19 years using harmonic constants derived from a minimum of one-year observations or by other proven methods known to give reliable results. A minimum period of 19 years, coincident with the Metonic cycle, is chosen because tide predictions are very similar at 19-year intervals (Pugh et al., 2014). However, some works have shown that in some regions the lowest astronomical tide occurs in periods exceeding 19 years. Hansen et al. (2015) detected in the Eastern

North Sea to Central Baltic Sea region, the highest astronomical tidal range in 74.4 and 55.8 year periods, which are multiplies of 18.6 year modulation cycles. Haigh et al. (2011) suggested that regions where the 18.6-year nodal tide modulations are largest occur in areas where large diurnal tides form and range over 4 m. It also shows that in regions where the semidiurnal tide exceeds 6 m, the 4.4-year cycle becomes more important. These variations are mainly related to the response of each basin to astronomical forcing. Different geographies, continental shelves and latitudes generate different tidal types in each place. The LAT is not easy to determine in terms of the tidal harmonic components. If each amplitude is added up (which would be the case when all the components are in phase), values would be too extreme since the components are not physically independent (Pugh et al., 2014). An example of this dependence occurs when the semi-diurnal components are slightly reduced if the diurnal components are larger. One of the problems that makes CD calculation difficult is that it varies both spatially and temporally. Likewise, the need for accurate harmonic constants over large regions of the ocean and with a homogeneous spatial distribution has only been resolved with the advent of satellite observations. These observations have made it possible to obtain sea height series of more than 27 years duration, leading to the development of global astronomical tide models and the possibility of obtaining astronomical tidal constants through harmonic analysis in the global ocean, as has been done by the Centre for Topographic studies of the Oceans and Hydrosphere (CTOH) (http://ctoh.legos.obs-mip.fr/). A great number of human activities require precise knowledge of the LAT, and if this is also referenced to the same reference system used by global navigation satellite systems, the WGS84 ellipsoid, important benefits are obtained. Some of these benefits include decreasing the cost and increasing the efficiency of hydrographic surveying, enabling the integration of data over the land/sea interface, and potentially contributing to precise navigation in critical areas (Turner et al., 2013). In the case of nautical charts, the depths that they provide are calculated as the distance between the seabed topography and the CD. These depths are obtained from soundings that must be corrected for several factors, such as the tidal correction, which is traditionally estimated from sea level observations in locations near or within the bathymetric survey area, stands out due to its magnitude. Obtaining the tidal correction through the ellipsoidal height of the water level provided by the global satellite navigation systems requires that the CD is also referenced to the ellipsoid, simplifying the calculation and improving the accuracy of the tidal correction applied to the depth soundings (Oreiro et al., 2016) (Figure 1). There are programs that link the CD to the ellipsoid, such as: VDATUM in the United States (Myers et al. 2005), AUSHYDROID in Australia (Martin and Broadbent 2004), BLAST for the North Sea (Slobbe et al. 2013) and VORF for UK and Irish waters (Iliffe et al. 2007).

Accurate knowledge of the LAT may also be required in various oceanic endeavors, for example, offshore wind power installations, in the case of needing international industry certification, knowledge of the LAT is required to reference tidal levels (Ko et al., 2017). The LAT is also necessary for the installation of oil platforms or different means of obtaining marine energy.

The aim of this work is to calculate a 5km x 5km empirical model of LAT surfaces for a region of the Southwest Atlantic Ocean between latitudes 36°S and 54°S and longitude 54°W, referenced to the WGS84 ellipsoid. This model is calculated using mean sea level surfaces obtained from model results such as MSS CNES CLS15 (https://www.aviso.altimetry.fr/en/data/products/auxiliary-products/mss/mss-description.html) and DTU10MSS (https://www.space.dtu.dk/english/research/scientific_data_and_models/global_mean_sea_surface). Although the MSS CNES CLS15 model used a longer data series for its development than the DTU10MSS model, both being global models, they do not always perform in the same way in all regions. Furthermore, given that the study domain is quite large and presents dynamic particularities, we tested which of these models best fits the study region. For this purpose, satellite observations are used where the astronomical tide is corrected using predictions calculated with harmonic constants provided by CTOH. The same harmonic constants are used to calculate the LAT from predictions made for a 75-year period.
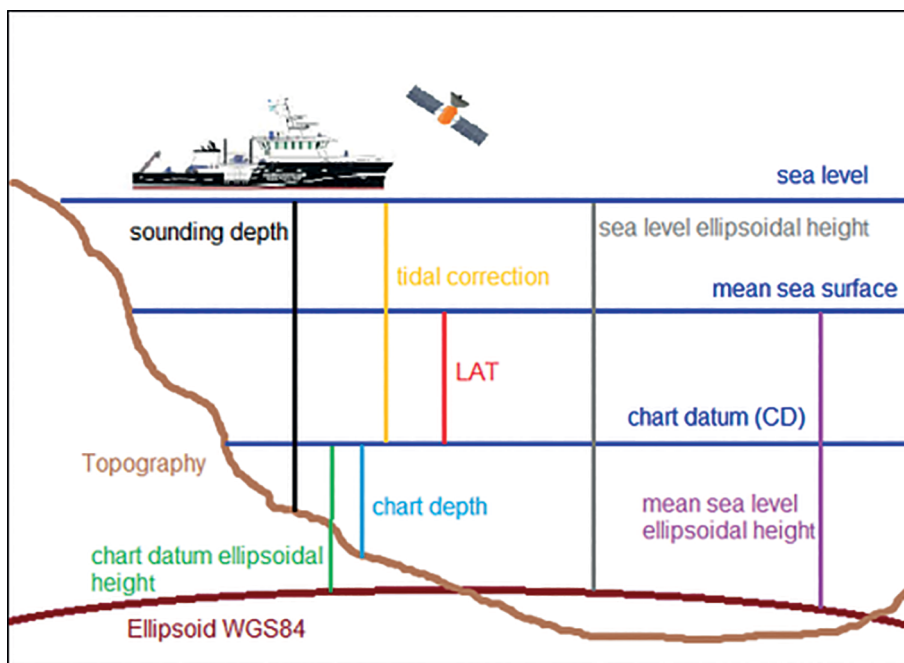
**Figure 1.** Diagram of the main surfaces and distances involved in a sounding measure.

## METHODS

### GLOBAL MEAN SEA LEVEL MODELS

The DTU10MSS global mean sea level model is the updated version of the DNSC08MSS model created by the DTU Space – National Space Institute (Andersen et al., 2010). This model uses 17 years (1993-2009) of satellite altimetry measurements from ERS, Topex/Poseidon (T/P), Jason1 (J1), ICESAT and ENVISAT missions. The DTU10MSS model incorporates new geophysical corrections with respect to the previous version, including the dynamic atmosphere correction obtained from the MOG2D_IB model, and the ocean tide correction obtained with the GOT4.7 model (Andersen, 2010). The DTU10MSS model is distributed in ASCII format on a regular 1' x 1' grid, in the reference system used by T/P, J1 and Jason2 (J2) satellite altimeters (http://www.space.dtu.dk/english/Research/Scientific_data_and_models/downloaddata).

The MSS CNES CLS15 model is the updated version of the MSS CNES CLS11 and is based on 1 Hz measurements of sea level height made by different altimeters. It was created by Collecte Localization Satellites (CLS) and distributed by Archiving, Validation and Interpretation of Satellite Oceanographic data (AVISO), with the support of Centre National d'Etudes Spatiales (CNES). It utilizes

21 years of satellite altimetry measurements, referenced to the TOPEX ellipsoid. Table 1 summarizes the satellite missions and periods used to generate the MSS CNES CLS15 model (Pujol et al., 2018). The data resolution of this model is also 1'x 1'.

### HARMONIC CONSTANTS

The 73 harmonic constants (Table 2) provided by the CTOH are used in this work, called X-TRACK Coastal products (https://www.aviso.altimetry.fr/en/data/products/sea-surface-height-products/regional/x-tracksla.html), in the 6065 positions included in the study domain (Figure 2), to obtain astronomical tide predictions. These constants belong

**Table 1.** Satellite missions and periods used to generate MSS CNES CLS15 model.

| Satellite | Time period |
|---|---|
| T/P + Jason 1 + Jason 2 | 1993-2012 |
| T/P interleaved + Jason 1 interleaved | Sep 2002-Oct 2005 and Feb 2009-Mar 2012 |
| Ers 2 + Envisat | May 1995-Oct 2010 |
| GFO | 2001-Aug 2008 |
| ERS 1 geodetic | Apr 1994-Mar 1995 |
| Cryosat 2 | 2011-May 2014 |
| Jason 1 geodetic | May 2012-Jun 2013 |

**Table 2.** Harmonic components provided by CTOH.

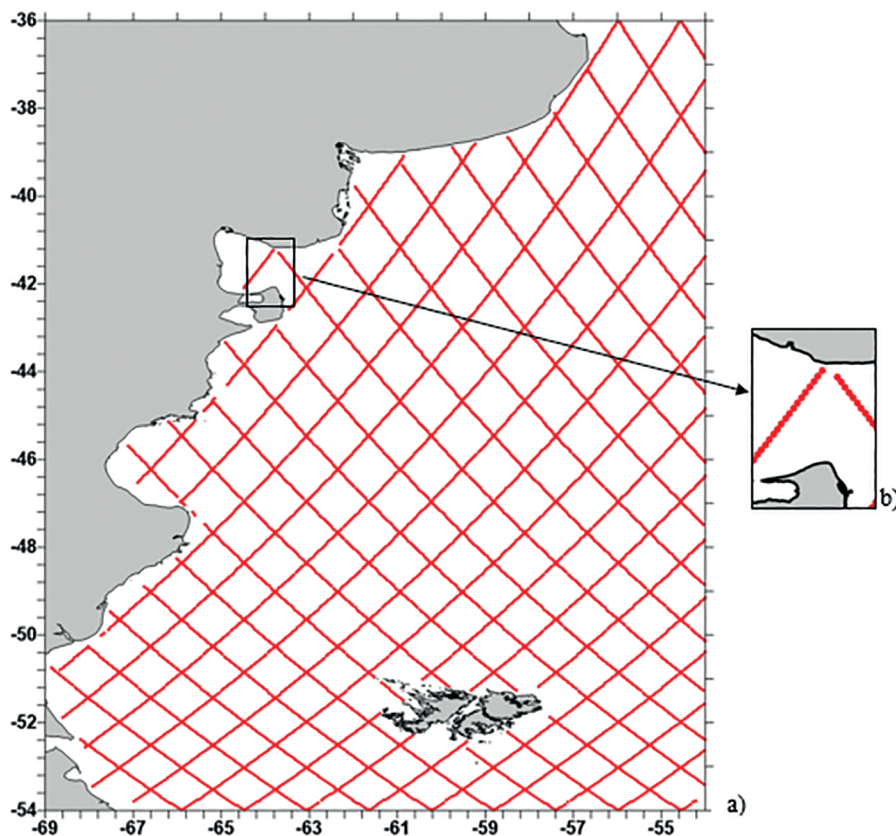| Constituents | | | |
|---|---|---|---|
| **Diurnal** | **Semidiurnal** | **Short period** | **Long period** |
| $2Q_1$, $Sig_1$,$Q_1$, $Ro1$,$O_1$, $MP_1$, $M_1$, $Ki_1$, $Pi_1$, $P_1$, $K_1$, $Psi_1$, $Phi_1$, $Tta_1$, $J_1$, $SO_1$, $OO_1$, $KQ_1$ | $OQ_2$, $MNS_2$, $E_2$, $2MK_2$, $2N_2$, $Mu2$, $N_2$, $Nu_2$, $MSK_2$, $M(SK)_2$, $M_2$, $M(KS)_2$, $MKS_2$, $La_2$, $L_2$, $T_2$, $S_2$, $R_2$, $K_2$, $MSN_2$, $KJ_2$, $2SM_2$ | $2MK_3$, $M_3$, $SO_3$, $MK_3$, $S_3$, $SK_3$, $N_4$, $3MS_4$, $MN_4$, $M_4$, $SN_4$, $MS_4$, $MK_4$, $S_4$, $SK_4$, $2MN_6$, $M_6$, $MSN_6$, $2MS_6$, $2MK_6$, $2SM_6$, $MSK_6$, $3MS_8$ | Sa, Ssa, MSm, Mm, MSf, Mf, MStm , Mtm, MSqm, Mqm, |



**Figure 2.** a) Study domain and locations (6065), where the astronomical tide predictions are calculated using harmonic constants provided by the CTOH. b) Enlargement of Figure 2 a) where the locations of the satellite observations along the traces can be seen in greater detail.

to the Atlantic Zone of South America. The improvements of the X-TRACK product and the gain in accuracy of nearshore data are analyzed and described by Birol et al., (2016), which motivates the use of this product among different existing global tide models. The positions of the locations with CTOH harmonic constant data are evidently coincident with those of the satellite observations, which allows to remove the astronomical tide from these observations without interpolating the values, to calculate the mean observational sea level (MOSL), and subsequently use these results when comparing the global mean sea level models.

## Satellite observations

To compare the global mean sea level models and choose the one that best fits the study region, the along-track sea level data provided by AVISO+ (https://www.aviso.altimetry.fr/) is used for the dates coinciding with those used to develop the mean sea level models to be compared. DTU10MSS model values are compared with satellite observations from 1993 to 2009, while MSS CNES CLS15 model values are compared with satellite observations from 1993 to 2013. These observations correspond to the TP, J1 and J2 missions. Observations on both main and interleaved tracks are considered. The tide-corrected

observational sea height (TOSH) is calculated according to Equation (1).

TOSH = *SLA*(*AVISO*) + *Tide*(*AVISO*) + *Mean Sea Level*(*AVISO*)
   - *Tide prediction calculated with CTOH constants*
   Equation (1)

These series of heights from satellite altimeters have a sampling interval of 9.9156 days, which does not remain constant between consecutive data due to missing observations for anomalous measurements or when using heights corresponding to a crossing of traces. These heights have the disadvantage that they are not observed in exactly the same position in each pass of the satellite, which can vary by 1 km (Chelton et al., 2001). To resolve the difference in the satellite observation position, we consider the heights inside circles of 1 km radius centered on the chosen position (the one reported by CTOH for the harmonic constants), for each model (Figure 3). The barycenter of these observations is then calculated and the original theoretical position is redefined and used to compare the MOSL and that of each mean sea level model. The MOSL is obtained by calculating the arithmetic mean of the TOSH values included in each circle of each model. By averaging the values, the anomalies present in the TOSH data are attenuated.

## LOWEST ASTRONOMICAL TIDE

For the calculation of the LAT, it was decided to use 75 years of hourly astronomical tidal predictions, given the large extent of the study area and the lack of precise knowledge for each location about the importance of a nodal cycle greater than the Metonic one. This period is arbitrarily chosen from 1/1/1990 to 12/31/2064. In addition, tidal predictions are calculated to coincide with the dates on which there are satellite observations in the development period corresponding to each mean sea level global model.

Equation (2) is used to calculate the predictions, which does not include the angular velocity of the tidal components, thus making predictions of more
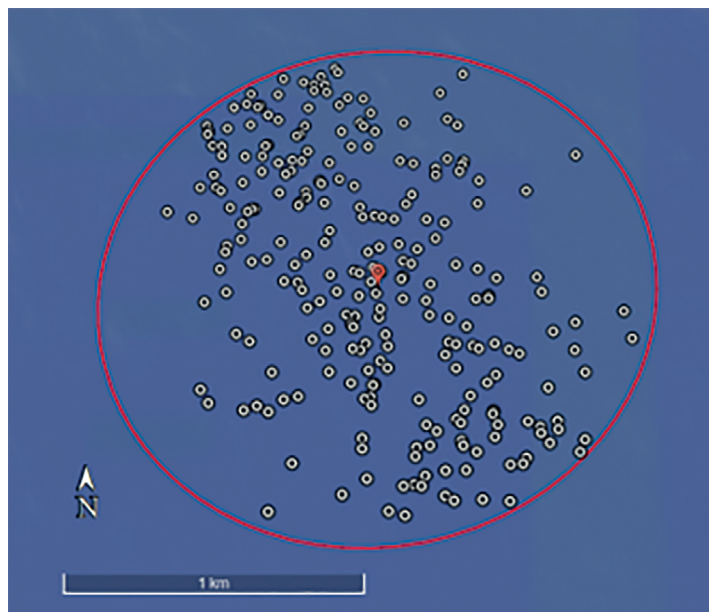


**Figure 3.** Location of the satellite observations corresponding to the period used in the development of the global mean sea level model MSS CLS15, within a circle of 1 km radius, with center at the position reported by CTOH for its harmonic constants (marked in red, located at coordinates 43°23'24 "S and 64°51'33 "W).

than one-year duration more accurate, since the nodal factor and the equilibrium argument are recalculated for each height. When the angular velocity is used, it is convenient to extend the prediction to a maximum of 1 year, since the variation of u is not taken into account (Oreiro et al., 2014 and D'Onofrio et al., 2016).

$$h(t) = \Sigma_{j=1}^{n} H_j.f_f.\cos((V+u)_j - g_j) \quad \text{Equation (2)}$$

where h(t) is the predicted tidal height at time t, where t is the observation time, $H_j$ the harmonic constant amplitude of the j component, $f_j$ the nodal factor of the j component at time t, $(V+u)_j$ the equilibrium argument of the j component at time t, $g_j$ the modified epoch of the j component and n the number of tidal components used. The equilibrium arguments and nodal factors are calculated considering the new time scales presented by Cartwright (1985).

### Comparison of global mean sea level models

To decide which model best fits the region, the models are compared with the MOSL obtained for the position of the barycenter of the observations. The gridded data from each model are interpolated to the coordinates of each barycenter and the mean sea level for each location is obtained. The arithmetic mean and standard deviation of the difference between the value of each model and the corresponding MOSL is calculated for all positions, and the model with the smallest standard deviation is chosen.

Finally, to calculate the correction needed to convert the mean level heights referenced to the TOPEX ellipsoid into heights referenced to the WGS84 ellipsoid (Table 3), the program "ICESat/GLAS and WGS-84 ellipsoid and geoid conversions" (Di Marzio, 2007) is used.

Since the differences in elevations between these ellipsoids are so small as latitude varies, it is possible to approximate the change in elevation between ellipsoids for a given latitude using the empirically calculated Equation (3) (Haran T.,2004):

$$\Delta h = h_2 - h_1 = -((a_2 - a_1) * \cos (\varphi)^2 + (b_2 - b_1) * \sin(\varphi)^2) \quad \text{Equation (3)}$$

where $\varphi$ is the latitude, $h_1$ y $h_2$ are the elevations of ellipsoids 1 and 2, $a_1$ and $a_2$ are the equatorial radius of ellipsoids 1 and 2 and $b_1$ and $b_2$ are the polar radius of ellipsoids 1 and 2, respectively. This equation greatly simplifies the calculation of the change in elevation compared to the exact method.

### Calculation of CD surfaces

Once the predictions have been made, the LAT is calculated by determining the lowest hourly height and the two heights before and after it for each prediction. A cubic spline is adjusted to these 5 heights to determine the lowest point that represents the LAT.

To obtain the CD referred to the WGS84 ellipsoid, the LAT value obtained in each position is subtracted from each mean sea level value, already referenced to WGS84. The geographic coordinates of each point of the domain are transformed to planar coordinates Gauss-Krüger Argentina zone 4, and then proceed to the interpolation of the distances of the CD to the WGS84 ellipsoid.

From this interpolation a 5km x 5km grid is obtained with the distances between the CD and the WGS84 ellipsoid. To perform this interpolation, different methods are tested: minimum curvature, Kriging, inverse of the weighted distance, modified Shepard, nearest neighbor, radial basis function and triangulation with linear interpolation. The Kriging method is chosen, as it presents the lowest mean squared error of the differences between the lowest tide heights obtained for the positions of the sea level height series and the corresponding ones for those positions, calculated by interpolation between the values of the grid nodes.

### Results

#### Selection of the mean sea level model

The arithmetic mean and standard deviation values calculated for each model with respect to the observational data are shown below (Table 4). As can be observed, the lowest standard deviation value corresponds to the MSS CLS15 model, which is why this model was chosen to refer the CD data to the WGS84 ellipsoid.

**Table 3.** Characteristics of Topex and WGS84 ellipsoids.

| Characteristics | TOPEX | WGS84 |
|---|---|---|
| Equatorial radius (a), [m] | 6378136.3 | 6378137 |
| Polar radius (b), [m] | 6356751.601 | 6356752.314 |
| Flattening (1/f) | 1/298.25700000 | 1/298.25722356 |

**Table 4.** Results of the calculation of the mean value and standard deviation of the DTU10MSS and MSS CLS15 models referenced to the observational data.

| Model | Mean value (m) | Standard deviation (m) |
|---|---|---|
| **DTU10MSS** | -0.0259 | 0.0222 |
| **MSS CLS15** | -0.0397 | 0.0177 |

It is important to mention that standard wave-form tracking systems aboard altimetry satellites do not provide reliable sea level information at a distance of less than 20-25km from shore. Even when the most advanced tracking systems are used, the gap in data coverage can still be a few kilometers (e.g., Deng et al. 2002; Sandwell and Smith 2005; Deng and Featherstone 2006). Because of this, the results of mean sea level models are less reliable in the vicinity of the coasts. Moreover, there is not enough mean sea level data for the coastal region from permanently installed tide gauges referenced to the ellipsoid. Figure 4 shows the mean sea level obtained from the MSS CLS15 global mean sea level referenced to the WGS84 ellipsoid.

## LAT AND CD SURFACES REFERENCED TO WGS84 ELLIPSOID

The results of the LAT calculations, referring to a mean sea level of 0m, are presented in Figure 5. These values were obtained from astronomical tide predictions made for a period of 75 years, with harmonic constants provided by CTOH. For better visualization, the values obtained at the grid points were interpolated using the Kriging method. Figure 5 shows the large range of the tide over the Patagonian shelf, with the greatest distances between the LAT and the mean level of 6.4m. It can also be seen how these distances gradually decrease in an offshore direction until reaching less variable values in a big area outside the shelf.

Finally the CD referenced to the WGS84 ellipsoid are presented in Figure 6. Due to the inaccuracy of the mean level values in the 20-25 km band from the coast, the surfaces represented are considered accurate from the mentioned distance. Following the recommendations of the IHO for the choice of the CD, curves of equal value with an equidistance of 0.3m

were determined. It is important to note that some meteorological conditions can result in water levels below the LAT, especially in shallow waters (Slobbe et al., 2013); therefore in these regions the effects of negative storm surges can be significant.

## DISCUSSION

In this work, the use of satellite heights, the harmonic constants provided by the CTOH and the results of mean sea level global models, allowed the development of an empirical model of the distances between the CD and the WGS84 ellipsoid for a region of the Southwest Atlantic Ocean where there are very few sea height observations in situ. The developed model has a resolution of 5km x 5km and covers the region between 36°S and 54°S and 54°W. As mentioned above, having the distance between the LAT and the WGS84 ellipsoid is essential for modern bathymetric surveys using the RTK (Real Time Kinamatic) method for both vessel positioning and water level measurement. The RTK method measures the water level below the vessel more accurately than a tide pole or tide gauge, because it takes into account the variations of the tide as well as the vessel draft during navigation (Scarfe, 2006). In addition, since the bathymetry may also be referenced to the WGS84 ellipsoid, the integration of the topography of the seabed and the coastal zone is achieved.

The referred satellite products have constituted the raw material of this work, and in particular the improvement introduced by LEGOS by reprocessing the data with coastally-oriented algorithms (Cancet et al., 2009), has allowed LAT surface values to be obtained even near shore. This is not the case with global mean sea level models as the errors near the coast can be on the order of one meter in the study region. However, the comparison of the two mean sea level models used with satellite data showed similar standard deviations. In the future, having information from the SHN coastal tide gauge network is expected, which at present consists of only 6 gauges for the study area: San Clemente, Mar del Plata, Quequén, Puerto Madryn, Puerto Belgrano and Puerto Deseado (http://www.hidro.gov.ar/oceanografia/mareografos.asp).
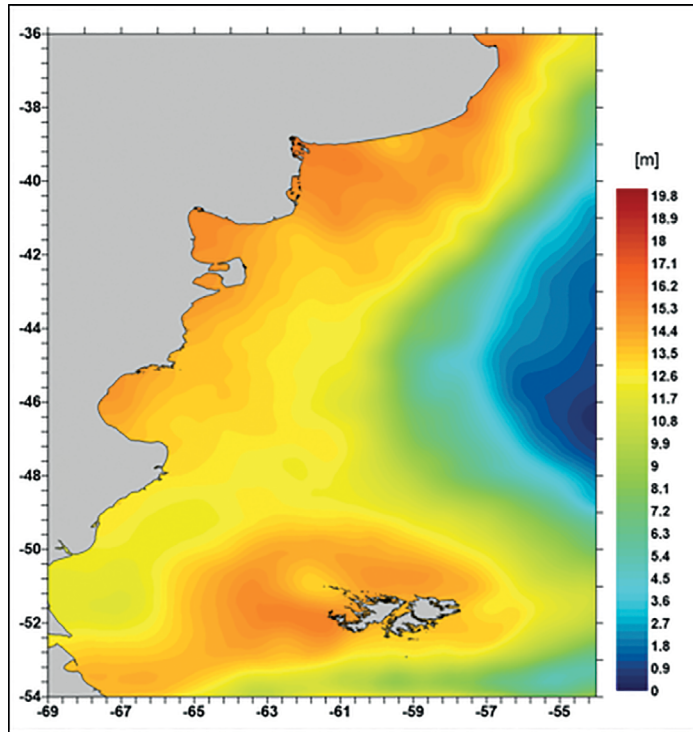
**Figure 4.** Mean sea level referenced to the WGS84 ellipsoid, obtained from the MSS CLS15 global mean sea level model data.
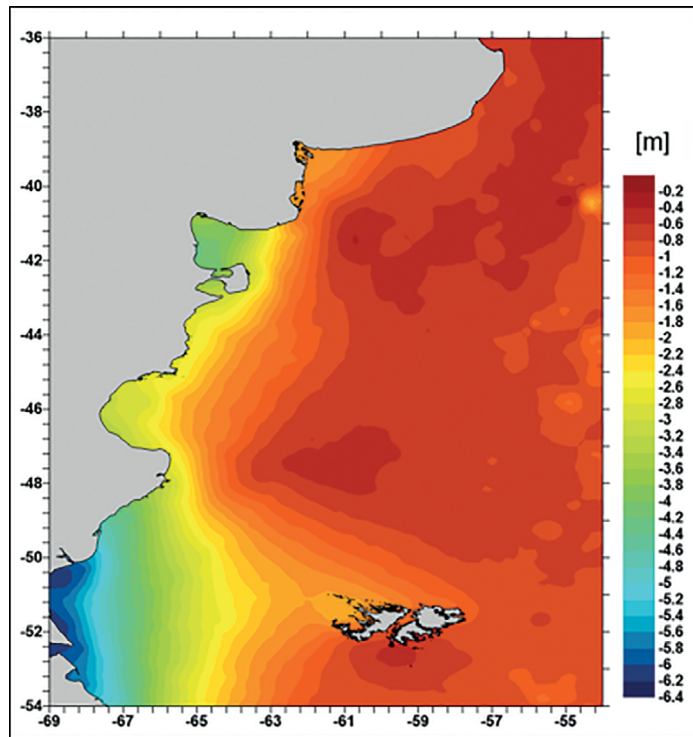


**Figure 5.** LAT (Lowest Astronomical Tide) surfaces, referred to the mean sea level 0m, calculated from 75-year predictions obtained with harmonic constants provided by the CTOH.
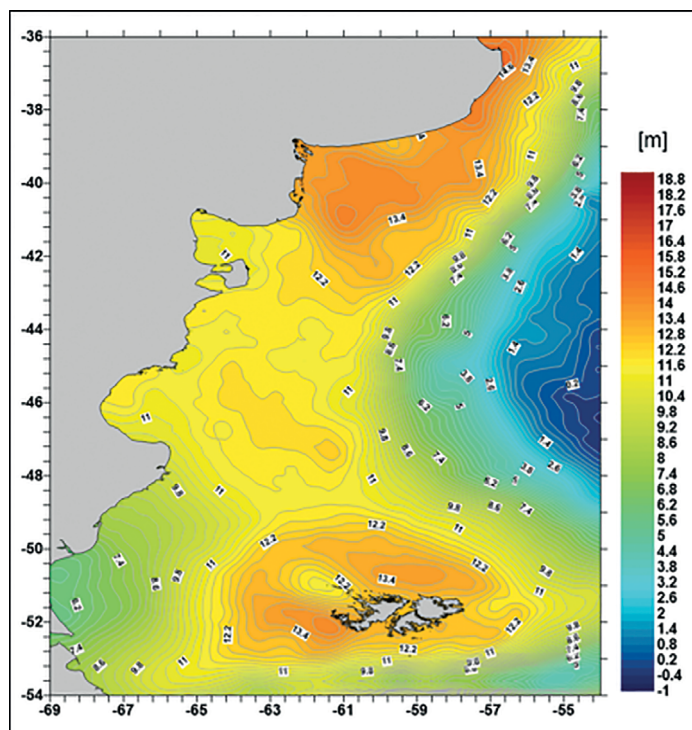
**Figure 6.** LAT (Lowest Astronomical Tide) referenced to WGS84 ellipsoid. Contours are delineated every 0.3m.

This work is the first empirical model for this area, characterized by tidal ranges that can exceed 10 m (D'Onofrio et al., 2016), among the largest in the global ocean. This characteristic is due to the fact that the width of the shelf is comparable with a quarter wavelength of a semidiurnal tidal wave, thus resulting in a near-resonant natural system (Buchwald, 1980). However, this is a first step, since, as mentioned above, the modeling of the coastal zone remains to be performed. To overcome this drawback, it is necessary to have sufficient *in situ* sea level observations referenced to the WGS84 ellipsoid or for global mean sea level models to increase their accuracy in the vicinity of the coasts. Moreover, regions close to islands, such as the one surrounding Isla de los Estados or the Malvinas Islands should be modeled at a higher spatial resolution. The tide in those places not only presents an important range as in the rest of the domain, but also, given the local dynamics, there are variations that are not observed at this scale of analysis. The tidal wave propagating from the south of the domain encounters the obstacle of Isla de los Estados and splits into two branches. One advances through

Le Maire Strait and the other through the eastern end of the island, with both branches meeting to the north of the island (Glorioso et al., 1997). This causes a gradient in the tidal range on a spatial scale that is not possible to detect at the resolution used in this work. Similarly, in the region of the Malvinas Islands where the abrupt shelf slope interrupted to the east of the Malvinas Islands by the Malvinas Plateau, the coexistence of the four tidal regimes defined according to the parameters established by Courtier has been found. It has been possible to also establish that the range of the semi-diurnal wave M2, which predominates in the region, varies between approximately 0.01 m and 1.10 m (Banegas, 2019). The results presented here are useful for the development of activities with great relevance in the area such as offshore hydrocarbon exploration and exploitation (de Haro, 2017) and shelf fishing associated with the presence of fronts that increase primary and secondary production (Olson and Backus, 1985). It is also of importance when considering the activities necessary to obtain marine energies given the untapped potential that the region has in this field.

## ACKNOWLEDGMENTS

## AUTHOR CONTRIBUTIONS

M.F.D.A.: Conceptualization, Investigation, Methodology, Software, Writing - Original draft, Writing - Review & editing.

E.E.D.: Conceptualization, Investigation, Methodology, Software, Writing - Review & editing.

L.B: Writing - Review & editing.

## REFERENCES

ANDERSEN, O. B. 2010. The DTU10 gravity field and mean sea surface. *In: Proceedings of Second International Symposium of the Gravity field of the Earth (IGFS2)*, 24 June, Fairbanks, Alaska, DTU Space – National Space Institute.

BANEGAS, L. 2019. *Estudio de la dinámica de marea en la región de las Islas Malvinas y Namuncurá/Banco Burdwood.* DSc. Buenos Aires: Facultad de Ciencias Exactas y Naturales, Universidad de Buenos Aires.

BIROL, F., FULLER, N., LYARD, F., CANCET M., NIÑO F., DELEBECQUE C. & FLEURY, S. 2017. Coastal applications from nadir altimetry: example of the X-TRACK regional products. *Advances in Space Research,* 59(4), 936-53, DOI: https://doi.org/10.1016/j.asr.2016.11.005

BUCHWALDV, V. T. 1980. Resonance of Poincar'e waves on a continental shelf. *Australian Journal of Marine and Freshwater Research,* 31(4), 451-457.

CANCET, M., BIROL, F., ROBLOU, L., LANGLAIS, C., GUIHOU, K., BOUFFARD, J., DUSSURGER, R., MORROW, R. & LYARD, F. 2014. CTOH regional altimetry products: examples of applications. *Coastal Altimetry* [online], 9, 1-5. Available at: https://www.researchgate.net/publication/251236986 [Accessed 17 Mar. 2021].

CARTWRIGHT, D. E. 1985. Tidal prediction and modern time scales, *International Hydrographic Review,* 62(1), 127-138.

CHELTON, D. B., RIES J. C., HAINES, B. J., FU, L. L. & CALLAHAN, P. S. 2001. Satellite altimetry and earth sciences: a handbook of techniques and applications. *In:* FU, L. L. & CAZENAVE, A. (eds.). *International geophysics series.* San Diego: Academic Press.

DENG, X. & FEATHERSTONE, W. E. 2006. A coastal retracking system for satellite radar altimeter waveforms: application to ERS-2 around Australia. *Journal of Geophysical Research: Oceans,* 111(C6), 1-16, DOI: https://doi.org/10.1029/2005JC003039

DENG, X., FEATHERSTONE, W. E., HWANG, C. & BERRY, P. A. M. 2002. Estimation of contamination of ERS-2 and POSEIDON satellite radar altimetry close to the coasts of Australia. *Marine Geodesy*, 25(4), 249-271.

D'ONOFRIO, E. E., OREIRO, F. A., GRISMEYER, W. H. & FIORE, M. M. E. 2016. Predicciones precisas de marea astronómica calculadas a partir de altimetría satelital y observaciones costeras para la zona de Isla Grande de Tierra del Fuego, Islas de los Estados y Canal de Beagle. *GeoActa,* 40(2), 60-75.

DI MARZIO, J. P. 2007. *GLAS/ICESat 500 m laser altimetry digital elevation model of Antarctica, Version 1. Appendix a: how does the Glas ellipsoid compare with WGS84 (by Terry Haran 20 May 2004).* Colorado: NASA National Snow and Ice Data Center, DOI: https://doi.org/10.5067/K2IMI0L24BRJ

GLORIOSO, P. D. & FLATHER, R. A. 1997. The Patagonian shelf tides. *Progress in Oceanography,* 40(1-4), 263-283.

HAIGH, I. D., ELIOT, M. & PATTIARATCHI, C. 2011. Global influences of the 18.61 year nodal cycle and 8.85 year cycle of lunar perigee on high tidal levels. *Journal of Geophysical Research*, 116(C6), 1-16, DOI: http://dx.doi.org/10.1029/2010JC006645

HANSEN, J. M., AAGAARD, T. & KUIJPERS, A. 2015. Sea-level forcing by synchronization of 56- and 74-year oscillations with the Moon's nodal tide on the northwest European Shelf (eastern North Sea to central Baltic Sea). *Journal of Coastal Research,* 31(5), 1041-1056.

HARO, C. 2017. Actividad hidrocarburífera off shore y prospecciones sísmicas en la Argentina. Impactos en la fauna marina, acciones de prevención y mitigación. *Fronteras,* 2017(15), 61-69.

ILIFFE, J. C., ZIEBART, M. K. & TURNER, J. F. 2007. The derivation of vertical datum surfaces for hydrographic applications. *The Hydrographic Journal,* 125, 3-8.

IOH (International Hydrographic Organization). 2018. *Resolutions of the International Hydrographic Organization*. 2nd ed. Monaco: International Hydrographic Organization.

KO, D. H., JEONG, S. T., CHO, H. Y. & KANG, K. S. 2017. Analysis on the estimation errors of the lowest and highest astronomical tides for the southwestern 2.5 GW offshore wind farm, Korea. *International Journal of Naval Architecture and Ocean Engineering,* 10(1), 85-94, DOI: http://dx.doi.org/10.1016/j.ijnaoe.2017.03.004

MARTIN, R. J. & BROADBENT, G. J. 2004. Chart datum for hydrography. *The Hydrographic Journal,* 112, 9-14.

MYERS, E., WONG, A., HESS, K., WHITE, S., SPARGO, E., FEYEN, J., YANG, Z., RICHARDSON, P., AUER, C., SELLARS, J., WOOLARD, J., ROMAN, D., GILL, S., ZERVAS, C. & TRONVIG, K. 2005. Development of a national Vdatum, and its application to sea level rise in North Carolina. *In: Proceedings of the U.S. Hydrographic Conference*, 29-31 March, San Diego, California, U.S. Hydrographic Conference.

OHI (Organización Hidrográfica Internacional). 1988. *Especificaciones cartográficas de la OHI y reglamentos de la OHI para las cartas internacionales (INT) MP-004*. Monaco: Organización Hidrográfica Internacional.

OLSON, D. B. & BACKUS, R. H. 1985. The concentrating of organisms at fronts: a coldwater fish and a warm-core Gulf Stream ring. *Journal of Marine Research*, 43(1), 113-137.

OREIRO, F. A., D'ONOFRIO, E. E. & FIORE, M. M. E. 2016. Altimetric reference connection of nautical charts and WGS84 ellipsoid for the Río de la Plata. *GeoActa,* 40(2), 109-120.

OREIRO, F. A., D'ONOFRIO, E. E., GRISMEYER, W. H., FIORE, M. M. E. & SARACENO, M. 2014. Tide model output comparison in the Northern region of the Antarctic Peninsula using satellite altimeters and tide gauges data. *Polar Science,* 8(1), 10-23.

PUGH, D. & WOODWORTH, P. 2014. *Sea-level science: understanding tides, surges, tsunamis and mean sea-level changes.* New York: Cambridge University Press.

PUJOL, M. I., SCHAFFER, P., FAUGÈRE, Y., RAYNAL, M., DIBARBOURE, G. & PICOT, N. 2018. Gauging the improvement of recent mean sea surface models: A new approach for identifying and quantifying their errors. *Journal of Geophysical Research*: *Oceans,* 123(8), 5889-5911, DOI: https://doi.org/10.1029/2017JC013503

SANDWELL, D. T. & SMITH, W. H. F. 2005. Retracking ERS-1 altimeter waveforms for optimal gravity field recovery. *Geophysical Journal International,* 163(1), 79-89, DOI: https://doi.org/10.1111/j.1365-246X.2005.02724.x

SCARFE, B. E. 2002. Measuring water level corrections (WLC) using RTK GPS. *The Hydrographic Journal,* 2002(104), 17-23.

SLOBBE, D. C., KLEES, R., VERLAAN, M., DORST, L. L. & GERRITSEN, H. 2013. Lowest astronomical tide in the North sea derived from a vertically referenced shallow water model, and an assessment of its suggested sense of safety. *Marine Geodesy,* 36(1), 31-71, DOI: https://doi.org/10.1080/01490419.2012.743493

TURNER, J. F., ILIFFE, J. C., ZIEBART, M. K. & JONES, C. 2013. Global ocean tide models: assessment and use within a surface model of lowest astronomical tide. *Marine Geodesy,* 36(2), 123-137, DOI: http://doi.org/10.1080/01490419.2013.771717